STATUS OF VISCOUS HYDRODYNAMIC SIMULATIONS*

Kevin Dusling

Department of Physics, Brookhaven National Laboratory
Upton, New York 11973-5000, USA
and
Department of Physics and Astronomy, State University of New York
Stony Brook, NY 11794-3800, USA

(Received February 4, 2009)

In this paper I give an overview of the status of viscous hydrodynamic simulations performed by a number of groups. Also discussed is the use of electromagnetic observables as an alternative probe of the shear viscosity in heavy ion collisions.

PACS numbers: 25.75.Ld, 25.75.Cj

1. Introduction

There is a general consensus that the early matter produced at RHIC behaves as a near perfect fluid [1]. This conclusion was born out of the success of ideal hydrodynamic descriptions [2, 3] of both hadron transverse momentum spectra and elliptic flow measurements up to 1.5–2 GeV/c. Elliptic flow describes the anisotropy of particle production with respect to the reaction plane and is quantified by the measured v_2,

$$v_2 = \left\langle \frac{p_x^2 - p_y^2}{p_x^2 + p_y^2} \right\rangle . \tag{1}$$

Although it is too early to draw any definitive conclusions most likely the deviations from ideal hydrodynamic behavior can be ascribed to dissipative effects. This has already been suggested in some of the recent works on dissipative hydrodynamics [4–13].

In this paper I give an overview of the current status of 2+1 dimensional, boost-invariant, viscous hydrodynamic simulations. In the following section I discuss the hydrodynamic equations used by the various groups. Then I

* Presented at the IV Workshop on Particle Correlations and Femtoscopy, Kraków, Poland, September 11–14, 2008.

demonstrate the effect of viscosity on spectra and v_2. In the last section I discuss a separate topic; how electromagnetic probes can possibly help us learn about the viscosity of the matter produced in heavy ion collisions.

2. The hydrodynamic equations

In the following section I outline the equations of motion necessary for a second order description of viscous hydrodynamics. We start by summarizing the well known first-order Navier–Stokes theory. Then we outline the equations required for a second-order causal description of dissipative fluid dynamics.

2.1. 1st order viscous hydrodynamics — Navier–Stokes

Viscous hydrodynamics was originally formulated in the first-order Navier–Stokes approximation where the energy momentum tensor and baryon flux is a sum of their ideal and dissipative parts:

$$T^{\mu\nu} = \varepsilon u^\mu u^\nu + (p + \Pi)\Delta^{\mu\nu} + \pi^{\mu\nu}\,, \tag{2}$$

$$n^\mu = n u^\mu + j_{\rm d}^\mu\,, \tag{3}$$

where p, ε, n and $u^\mu = (\gamma, \gamma \boldsymbol{v})$ are the pressure, energy density, baryon density and four-velocity of the fluid. We use the convention that $g^{\mu\nu} = \mathrm{diag}(-1, +1, +1, +1)$ and therefore $u^\mu u_\mu = -1$. The dissipative terms, π and $j_{\rm d}$ depend on the definition of the local rest frame (LRF) of the fluid. A specific form of $\pi^{\mu\nu}$and v^μ can be found using the Landau–Lifshitz definition [14] of the LRF ($u_\mu \pi^{\mu\nu} = 0$), constraining the entropy to increase with time and by working within the Navier–Stokes approximation (keeping terms to first order in gradients only) resulting in

$$\pi^{\mu\nu} = -\eta \left(\nabla^\mu u^\nu + \nabla^\nu u^\mu - \frac{2}{3}\Delta^{\mu\nu}\nabla_\beta u^\beta \right)\,, \tag{4}$$

$$\Pi = -\zeta \nabla_\beta u^\beta\,, \tag{5}$$

$$j_{\rm d}^\mu = -\kappa \left(\frac{nT}{\varepsilon + p} \right)^2 \nabla^\mu \left(\frac{\mu}{T} \right)\,, \tag{6}$$

where κ, η and ζ are the heat conduction, shear and bulk viscosities of the fluid with temperature T and chemical potential μ. The viscous tensor is constructed with the differential operator $\nabla^\mu = \Delta^{\mu\nu} d_\nu$ where $\Delta^{\mu\nu} = g^{\mu\nu} + u^\mu u^\nu$ is the local three-frame projector, $d_\mu u^\nu = \partial_\mu u^\nu + \Gamma^\nu_{\gamma\mu} u^\gamma$ is the covariant derivative and $\Gamma^\nu_{\gamma\mu} \equiv 1/2 g^{\nu\alpha}(\partial_\mu g_{\alpha\gamma} + \partial_\gamma g_{\alpha\mu} - \partial_\alpha g_{\gamma\mu})$ are the Christoffel symbols.

The transport coefficients in a quark–gluon plasma and also in the hadronic gas were studied in Refs. [15–18]. It was found that the dominate dissipative mechanism was shear viscosity in both the QGP and hadronic gas. Bulk viscosity may however dominate in the transition region [19–21]. Heat transport can be ignored in the limit that $\mu_{\mathrm{B}} \ll T$ which is the limit taken here. In the following work we will consider viscous effects in a quark–gluon plasma phase only. For this purpose we consider a constant shear to entropy ratio, $\eta/s = \mathrm{const.}$, and a massless ideal gas, $p = 1/3\varepsilon$.

2.2. 2nd order viscous hydrodynamics

In order to render a second order theory it is necessary to introduce additional variables. These variables will relax on very short time scales to the standard thermodynamic quantities in the first order theory, but an evolution equation for them is still required in order to avoid acausal signal propagation. One such theory that has been used in a number of works was introduced by Israel and Stewart [22]. Instead we use a theory developed by [23, 24] due to its appealing structure when implemented numerically.

We now summarize the evolution equations used in the current analysis following the mathematical structure outlined in Ref. [24]. We use a simplified version of the model for deviations of the stress energy tensor close to equilibrium. The new dynamical variable that is introduced is the tensor variable $c_{\mu\nu}$ which will later be shown to be closely related to the velocity gradient tensor, $\pi_{\mu\nu}$. The tensor variable $c_{\mu\nu}$ is conveniently defined to have the property $c_{\mu\nu}u^{\nu} = u_{\mu}$ and for small deviations from local thermal equilibrium the energy momentum tensor is given in the local rest frame (LRF) by

$$T^{ij}_{\mathrm{LRF}} = p\left(\delta^{ij} - \alpha c^{ij}\right) , \tag{7}$$

where α is a small parameter related to the relaxation time. The equations of motion are dictated by conservation of energy and momentum, $d_{\mu}T^{\mu\nu} = 0$. In addition, an evolution equation for the generalized mechanical force tensor is needed [24]

$$u^{\lambda}(\partial_{\lambda}c_{\mu\nu} - \partial_{\mu}c_{\lambda\nu} - \partial_{\nu}c_{\mu\lambda}) = \frac{-1}{\tau_0}\,\overline{c}_{\mu\nu} - \frac{1}{\tau_2}\,\mathring{c}_{\mu\nu}\,, \tag{8}$$

where $\overline{c}$ and $\mathring{c}$ are defined as the isotropic and traceless parts of the tensor variable $c_{\mu\nu}$ defined as

$$\overline{c}_{\mu\nu} = \tfrac{1}{3}(c^{\lambda}_{\lambda} - 1)(\eta_{\mu\nu} + u_{\mu}u_{\nu})\,, \tag{9}$$

$$c_{\mu\nu} + u_{\mu}u_{\nu} = \mathring{c}_{\mu\nu} + \overline{c}_{\mu\nu}\,. \tag{10}$$

In the limit that the relaxation times (τ_0, τ_2) are very small the evolution equation yields

$$c^{ij} = \tau_2 \left(\partial_i u^j + \partial_j u^i - \tfrac{2}{3}\delta^{ij}\partial_k u^k\right) + \tfrac{2}{3}\tau_0 \delta^{ij}\partial_k u^k \,. \tag{11}$$

Substituting the above equation into $T^{ij}_{\rm LRF}$ and comparing the result to the Navier–Stokes equation (6) the bulk and shear viscosities can be identified

$$\begin{aligned} \eta &= \tau_2 p\alpha \,, \\ \zeta &= \tfrac{2}{3}\tau_0 p\alpha \,. \end{aligned} \tag{12}$$

Now let us briefly discuss the different formalisms used by various groups. The first simulations done by Song/Heinz and separately by Chaudhuri used the *simplified* Israel–Stewart (IS) equations [7, 8] which neglect terms of second order in the stress-energy tensor

$$\Delta^m_j \Delta^n_k \dot{\pi}^{jk} = -\frac{1}{\tau_\pi}(\pi^{mn} - 2\eta\sigma^{mn}) \,. \tag{13}$$

In principal all terms of second order in gradients should be treated on an equal footing and therefore included. Conformal invariance imposes constraints on these terms however [25]. This led to the second order equations used by Romatschke [6]

$$\Delta^m_j \Delta^n_k \dot{\pi}^{jk} = -\frac{1}{\tau_\pi}(\pi^{mn} - 2\eta\sigma^{mn}) + \frac{1}{2}\pi^{mn}\left(5D(\ln T) - \partial_k u^k\right) . \tag{14}$$

Then there is the *full* IS equations used by Song and Heinz [12]

$$\Delta^m_j \Delta^n_k \dot{\pi}^{jk} = -\frac{1}{\tau_\pi}(\pi^{mn} - 2\eta\sigma^{mn}) - \frac{1}{2}\pi^{mn}\frac{\eta T}{\tau_\pi} d_k \left(\frac{\tau_\pi}{\eta T} u^k\right) . \tag{15}$$

Finally, if we take the OG equations (used here and in [9]) and re-express them in terms of the IS stress energy tensor the equation of motion is

$$\begin{aligned} \Delta^m_j \Delta^n_k \dot{\pi}^{jk} \;&=\; -\frac{1}{\tau_\pi}(\pi^{mn} - 2\eta\sigma^{mn}) - \left[\frac{4}{3} + \frac{2}{3} - \frac{2\beta}{\alpha}\right]\pi^{mn}\partial_k u^k \\ &\quad + \pi_{\lambda(\mu}\omega^\lambda_{\nu)} + \frac{1}{\eta}\pi_{\lambda\langle\mu}\pi^\lambda_{\mu\rangle} \,, \end{aligned} \tag{16}$$

where β is a free parameter. For $\beta = \alpha/3$ the stress-energy tensor is Weyl invariant. There has been much progress in the way of a code comparison of the different viscous hydrodynamic results which has been initiated by the TECHQM and CATHIE collaborations. The preliminary results can be found on the respective wiki pages [26].

3. Results

3.1. Transverse momentum spectra and elliptic flow

In Fig. 1 we show transverse momentum spectra and the differential elliptic flow of gluons in Au–Au collisions at RHIC. The simulation was performed using an ideal equation of state down to the decoupling temperature of $T_{\mathrm{f.o.}} = 130$ MeV. Additional parameters of the simulation are shown in the figure text.

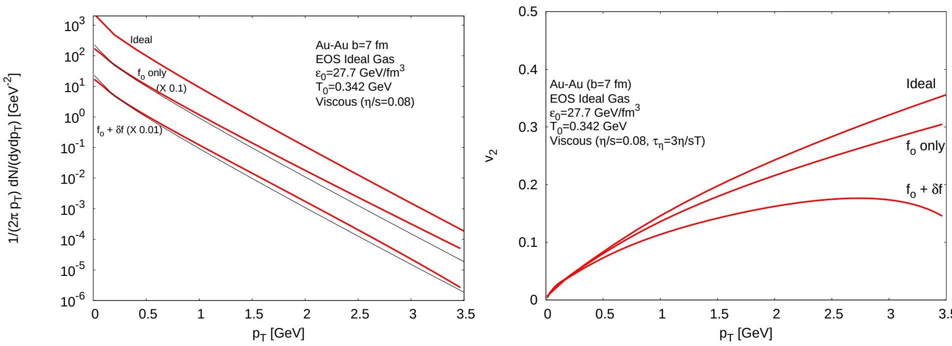

Fig. 1. Effect of shear viscosity on $p_\perp$ spectra (left) and $v_2(p_\perp)$ (right) of massless particles. The thin black curves in the left plot show the rescaled ideal result for comparison to the viscous result.

For both plots we show the ideal calculation as well as two viscous results. One which we call *flow only* (labeled as 'f_0 only') and a second, which is the true viscous result (labeled '$f_0 + \delta f$').

The flow only (f_0 only) shows the particle spectra when computed using the ideal particle distribution in the Cooper–Frye freezeout procedure. This procedure is thermodynamically inconsistent. When shear viscosity is present the particles' distribution functions deviate from their ideal form. By not including the proper viscous correction to distribution function energy-momentum conservation is violated when converting from hydro to particles. Therefore the curve labeled 'f_0 only' is useful for pedagogical purposes alone. It shows how the viscous correction to the ideal equations of motion manifests itself in the spectra.

The result $f_0 + \delta f$ is the viscous result to be contrasted with the ideal results. In this case the particle distribution in the Cooper–Frye formula includes its off-equilibrium correction

$$\delta f \propto \frac{1}{(\varepsilon + p)T^2} f_0(1 + f_0) p^\alpha p^\beta \pi_{\alpha\beta} \,. \tag{17}$$

3.2. Freezeout

In this section the freezeout criteria is discussed in more detail. Normally, in ideal hydrodynamic simulations, one uses a surface of constant temperature as the freezeout hyper-surface. Viscosity introduces an additional length scale into the problem which can be used to estimate when freezeout should occur. The condition for hydrodynamics to be applicable is that the relaxation time should be much smaller than the inverse expansion rate, $\tau_R \partial_\mu u^\mu \ll 1$. We define the following freezeout parameter

$$\chi = \frac{4}{T} \partial_\mu u^\mu \tag{18}$$

and the freezeout hyper-surface is constructed as a surface of constant χ as was done in [9].

Let us now compare the results from a constant temperature freezeout surface to one of constant χ. In Fig. 2 we show the integrated v_2 over eccentricity as a function of centrality (expressed as $1/S dN_{\rm ch}/dy$) where S is the transverse overlap area of the collision region. It was found in [27] that to a good approximation the dependence on system size, impact parameter and collision energy can be absorbed into how these parameters change the final multiplicity. See the paper by Song and Heinz [12] for a nice description of *multiplicity scaling* and the effect of viscosity on scaling violations.

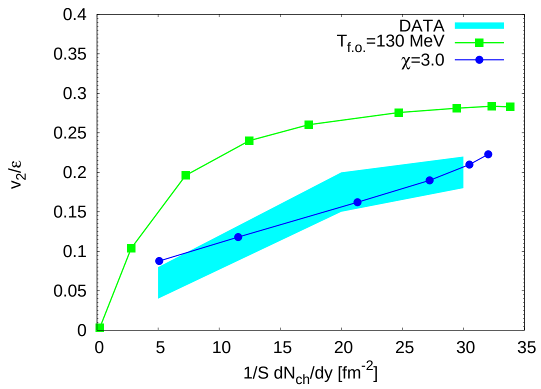

Fig. 2. v_2/ε as a function of centrality from hydrodynamic simulations using a constant temperature hypersurface ($T_{\rm f.o.} = 130$ MeV) *versus* a constant $\chi = 3$ freezeout surface. χ is a measure of the scattering time to the expansion rate.

Going back to Fig. 2 the grey (blue) band is indicative of the data from various experiments at different system sizes and beam energies. The upper (green) curve is the result using a constant temperature freezeout surface. This should be contrasted to the lower (blue) curve which uses a freezeout surface of constant χ. We find that by changing the freezeout criteria to a more natural one, $\chi = \text{const.}$, that the elliptic flow is closer to the data. A full analysis using a more realistic equation of state still needs to be done.

3.3. Dileptons

In this section I discuss how shear viscosity modifies the thermally produced dileptons. The leading order contribution to dilepton production comes for $q\overline{q}$ annihilation. From a kinetic theory point of view the rate is calculated from

$$\frac{dN}{d^4q} = \int \frac{d^3\boldsymbol{k}_1}{(2\pi)^3}\frac{d^3\boldsymbol{k}_2}{(2\pi)^3} f(E_1,T)f(E_2,T)v_{12}\sigma(M^2)\delta^4(q-k_1-k_2)\,, \tag{19}$$

where $q = (q_0, \boldsymbol{q})$ is the virtual photon's four momentum and $M^2 = (E_1 + E_2)^2 - (\boldsymbol{k}_1 + \boldsymbol{k}_2)^2$ is the photon's invariant mass. Throughout this work we consider massless quarks; therefore $E_{1,2} = \sqrt{\boldsymbol{k}_{1,2}^2 + m_q^2} \approx |\boldsymbol{k}_{1,2}|$. The function $f(E,T)$ is the quark or anti-quark momentum distribution function, which in thermal equilibrium is given by $f(E,T) = 1/(1 + e^{E/T})$.

As was discussed in the previous section, in the presence of viscosity the particles' distribution functions will no longer take on their equilibrium form. For massless fermions the correction is approximately given as

$$f(k) \to f_0(k) + \frac{1}{2(\varepsilon + p)T^2} f_0(k)[1 - f_0(k)]k^\alpha k^\beta \pi_{\alpha\beta}\,. \tag{20}$$

We can now substitute this viscous correction into the quarks distribution function of the kinetic theory expression (19). The phase space integrals can be done analytically in the limit of large mass dileptons (*i.e.* $M/T \gg 1$)

$$\frac{dN}{d^4q} = \frac{N_c\alpha^2 e_q^2}{12\pi^4} e^{-q_0/T}\left[1 + \frac{1}{3(\varepsilon + p)T^2} q^\alpha q^\beta \pi_{\alpha\beta}\right]\,. \tag{21}$$

The exact expression for any invariant mass is given in [28].

In order to compare the rates given above with those measured in experiment one must integrate the rates over the space-time history of the hydrodynamic evolution. This is done with the same hydrodynamic model discussed in the previous section. There are additional sources of dileptons beyond the simple $q\overline{q}$ annihilation just discussed. One must also include dileptons emanating from the hadronic phase as well. The dominant reaction is $\pi\pi \to \rho \to \mathrm{e}^+e^-$ but other processes contribute significantly as well. We therefore use the hadronic rates constrained by the chiral reduction formula [29], which takes into account many reactions beyond the leading $\pi\pi$ annihilation. These rates have been used to study the dimuons measured by the NA60 Collaboration [30, 31] as well as electron pairs measured by PHENIX at RHIC [32] using an ideal hydrodynamic model for the space-time evolution. In [33] we have gone beyond this and looked at the effect of viscosity. We now summarize these results.

The left plot of Fig. 3 shows the invariant mass spectrum of muon pairs as measured by NA60 [34–36]. The curves show the dimuon yields from $q\bar{q}$ annihilation in the plasma phase and using the CRF for the dilepton rates in the hadronic phase. The results for three different equation of states are shown. Two are for a second order phase transition having a latent heat of 0.3 and 1.2 GeV/fm^3. The second is an equation of state motivated by the lattice [37]. Even though they all give a reasonable description of the mass spectra they lead to very different $T_{\rm eff}$ as a function of mass. It turns out that LH $= 0.3$ GeV/fm^3 gives the best fit to the $T_{\rm eff}$ data. $T_{\rm eff}$ is defined by fitting the dilepton $p_\perp$ spectra to $\exp(-m_\perp/T_{\rm eff})$ at a given invariant mass.

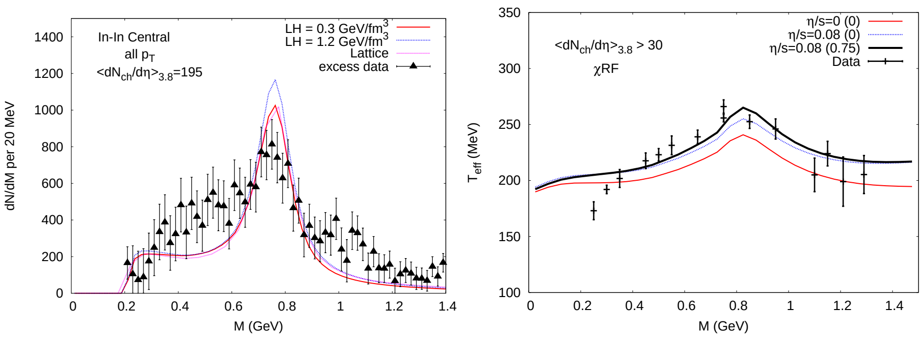

Fig. 3. (left) Dimuon invariant mass spectra *versus* hydrodynamic calculations. (right) $T_{\rm eff}$ spectra as measured by NA60 *versus* the hydrodynamic calculations for the ideal case $\eta/s = 0(0)$, shear viscosity in the *qgp* phase only $\eta/s = 0.08(0)$ and with additional viscosity in the hadronic phase $\eta/s = 0.08(0.75)$.

The right plot shows $T_{\rm eff}$ *versus* mass using the LH $= 0.3$ GeV/fm^3 EoS. Also shown are the results with $\eta/s = 0.08$ in the QGP phase and a hadronic phase having $\eta/s = 0$ and 0.75. The effect is clear. Shear viscosity brings about a *hardening* of the dilepton $p_\perp$ spectra thereby resulting in a larger $T_{\rm eff}$. We note that the effect of the hadronic viscosity is only seen near the ρ pole ($M \approx 0.770$ GeV) as this region is dominated by hadronic emission. At higher mass ($M \geq 1$ GeV) the emission is dominated by the QGP and the hadronic viscosity does not effect the spectra in this region.

I would like to thank my collaborators Derek Teaney and Shu Lin. This work is partially supported by the US-DOE grants DE-FG02-88ER40388, DE-FG03-97ER4014 and DE-AC02-98CH10886.

REFERENCES

[1] J.Y. Ollitrault, *Pramana* **67**, 899 (2006).

[2] D. Teaney, J. Lauret, E.V. Shuryak, `arXiv:nucl-th/0110037`; *Phys. Rev. Lett.* **86**, 4783 (2001).

[3] P.F. Kolb, U.W. Heinz, `arXiv:nucl-th/0305084`.

[4] R. Baier, P. Romatschke, *Eur. Phys. J.* **C51**, 677 (2007) `[arXiv:nucl-th/0610108]`.

[5] P. Romatschke, *Eur. Phys. J.* **C52**, 203 (2007) `[arXiv:nucl-th/0701032]`.

[6] P. Romatschke, U. Romatschke, *Phys. Rev. Lett.* **99**, 172301 (2007) `[arXiv:0706.1522 [nucl-th]]`.

[7] A.K. Chaudhuri, `arXiv:0708.1252 [nucl-th]`.

[8] H. Song, U.W. Heinz, *Phys. Lett.* **B658**, 279 (2008) `[arXiv:0709.0742 [nucl-th]]`.

[9] K. Dusling, D. Teaney, *Phys. Rev.* **C77**, 034905 (2008) `[arXiv:0710.5932 [nucl-th]]`.

[10] H. Song, U.W. Heinz, `arXiv:0712.3715 [nucl-th]`.

[11] P. Bozek, `arXiv:0712.3498 [nucl-th]`.

[12] H. Song, U.W. Heinz, *Phys. Rev.* **C78**, 024902 (2008) `[arXiv:0805.1756 [nucl-th]]`.

[13] M. Luzum, P. Romatschke, *Phys. Rev.* **C78**, 034915 (2008) `[arXiv:0804.4015 [nucl-th]]`.

[14] L.D. Landau, E.M. Lifshitz, *Fluid Mechanics*, Pergamon Press, London 1959.

[15] P. Danielewicz, M. Gyulassy, *Phys. Rev.* **D31**, 53 (1985).

[16] M. Prakash, M. Prakash, R. Venugopalan, G. Welke, *Phys. Rep.* **227**, 321 (1993).

[17] G. Baym, H. Monien, C.J. Pethick, D.G. Ravenhall, *Phys. Rev. Lett.* **64** (1990) 1867.

[18] P. Arnold, G.D. Moore, L.G. Yaffe, *J. High Energy Phys.* **0305**, 051 (2003) `[arXiv:hep-ph/0302165]`.

[19] D. Kharzeev, K. Tuchin, `arXiv:0705.4280 [hep-ph]`.

[20] G.D. Moore, O. Saremi, *J. High Energy Phys.* **0809**, 015 (2008) `[arXiv:0805.4201 [hep-ph]]`.

[21] H.B. Meyer, *Phys. Rev. Lett.* **100**, 162001 (2008) `[arXiv:0710.3717 [hep-lat]]`.

[22] W. Israel, *Ann. Phys.* **100**, 310 (1976); W. Israel, J.M. Stewart, *Phys. Lett.* **A58**, 213 (1976).

[23] M. Grmela, H.C. Öttinger, *Phys. Rev.* **E56**, 6620 (1997); H.C. Öttinger, M. Grmela, *Phys. Rev.* **E56**, 6633 (1997); H.C. Öttinger, *Phys. Rev.* **E57**, 1416 (1993).

[24] H.C. Öttinger, *Physica A* **254**, 433 (1998).

[25] R. Baier, P. Romatschke, D.T. Son, A.O. Starinets, M.A. Stephanov, *J. High Energy Phys.* **0804**, 100 (2008) [arXiv:0712.2451 [hep-th]].

[26] https://wiki.bnl.gov/TECHQM/index.php/Code_verification_for_viscous_hydrodynamics https://wiki.bnl.gov/hhic/index.php/Main_Page#Code_comparison_for_viscous_hydrodynamics

[27] S.A. Voloshin, A.M. Poskanzer, *Phys. Lett.* **B474**, 27 (2000) [arXiv:nucl-th/9906075].

[28] K. Dusling, S. Lin, *Nucl. Phys.* **A809**, 246 (2008) [arXiv:0803.1262 [nucl-th]].

[29] H. Yamagishi, I. Zahed, *Ann. Phys.* **247**, 292 (1996) [arXiv:hep-ph/9503413].

[30] K. Dusling, I. Zahed, arXiv:hep-ph/0701253.

[31] K. Dusling, D. Teaney, I. Zahed, *Phys. Rev.* **C75**, 024908 (2007) [arXiv:nucl-th/0604071].

[32] K. Dusling, I. Zahed, arXiv:0712.1982 [nucl-th].

[33] K. Dusling, arXiv:0901.2027 [nucl-th].

[34] R. Arnaldi *et al.* [NA60 Collaboration], *Phys. Rev. Lett.* **96**, 162302 (2006) [arXiv:nucl-ex/0605007].

[35] S. Damjanovic *et al.* [NA60 Collaboration], *Nucl. Phys.* **A783**, 327 (2007) [arXiv:nucl-ex/0701015].

[36] R. Arnaldi *et al.* [NA60 Collaboration], *Phys. Rev. Lett.* **100**, 022302 (2008) [arXiv:0711.1816 [nucl-ex]].

[37] M. Laine, Y. Schroder, *Phys. Rev.* **D73**, 085009 (2006) [arXiv:hep-ph/0603048].